

# Doping of ZnSe during molecular beam epitaxial growth using an atomic phosphorus source

L. C. Calhoun and R. M. Park<sup>a)</sup>

*Department of Materials Science and Engineering, University of Florida, Gainesville, Florida 32611*

(Received 5 June 1998; accepted for publication 30 September 1998)

Zinc selenide films were doped with phosphorus during molecular beam epitaxial (MBE) growth by employing a novel, valved, three-zone solid-source radio frequency (rf)-cracker unit manufactured by Oxford Applied Research (OAR). Optical emission spectroscopy analysis of the plasmas produced in the rf chamber of the unit showed that the apparatus was capable of generating a flux of atomic phosphorus. By suitably adjusting the operating conditions of the unit, phosphorus concentrations in ZnSe epilayers were varied over the range of  $1 \times 10^{16} \text{ cm}^{-3}$  to high- $10^{18} \text{ cm}^{-3}$ , in a highly controlled and reproducible fashion. Phosphorus atoms, in contrast to  $\text{P}_4$  molecules, were found to be highly chemically reactive at the growing ZnSe surface at a normal growth temperature (around 300 °C), and the OAR unit was found to be eminently suitable for the provision of atomic P for MBE growth. Doping using atomic P was found, at least in lightly to moderately doped ZnSe, to provide an acceptor state that gave rise to a neutral-acceptor bound exciton emission located at 2.7919 eV, in keeping with that of other substitutional acceptors in ZnSe. Also, compensation in atomic P doped ZnSe appears to occur by virtue of the formation of shallow donor states rather than via the production of deep level states, which dominate in the case of most of the previously reported phosphorus-doped ZnSe studies. © 1999 American Institute of Physics. [S0021-8979(99)08201-8]

## I. INTRODUCTION

Phosphorus has been considered to be a potential *p*-type dopant for ZnSe and related alloys for a number of years, and a variety of studies have been reported concerning ZnSe:P.<sup>1-12</sup> Phosphorus-doped ZnSe has commonly been reported to exhibit deep level states, and a lack of *p*-type conductivity associated with ZnSe:P has typically been ascribed to compensation as a consequence of these deep levels. With regard to molecular beam epitaxial (MBE) growth of ZnSe:P, there have been three reports in the literature, two of which involved the use of compound  $\text{Zn}_3\text{P}_2$  as the source of phosphorus.<sup>9,10</sup> The authors of those two studies reported strong deep-level defect related emission in the photoluminescence spectra recorded from their moderately to heavily doped material. More recently, however, Neu *et al.*<sup>12</sup> employed an atomic-phosphorus source during MBE growth of ZnSe:P and reported significantly diminished deep level emission intensities. With regard to these three reports, however, only DePuydt *et al.*<sup>10</sup> determined phosphorus concentrations in their ZnSe:P films, and the maximum phosphorus concentration reported was only  $1.8 \times 10^{17} \text{ cm}^{-3}$ . In addition, all three groups reported that their P-doped films were insulating. Consequently, concern has been raised with regard to the solid solubility of phosphorus in ZnSe and, of course, the issue of deep level formation by virtue of phosphorus incorporation.

The use of a plasma-generated flux of atomic species has been shown to be an effective method of doping II–VI compounds during MBE growth. Using a flux of atomic nitrogen

from an rf-generated plasma, Park *et al.*<sup>13</sup> first demonstrated the efficacy of this method by successfully doping ZnSe *p* type during MBE growth using a gas source rf cracker unit manufactured by Oxford Applied Research (OAR), Oxfordshire, U.K. A similar gas source rf cracker unit was successfully employed by Fan *et al.*<sup>14</sup> to dope ZnTe *p* type with nitrogen.

More recently, this approach has been extended to include the production of atomic species from solid elemental source material. For instance, Lugauer *et al.*<sup>15</sup> and Tournié *et al.*<sup>16</sup> have reported using a solid source rf cracker unit to generate a flux of atomic arsenic, and Neu *et al.*<sup>12</sup> have reportedly generated atomic phosphorus using a solid source rf cracker unit for ZnSe doping. These particular atom sources, however, are not ideally suited for high vapor pressure materials due to an inability to isolate the source material during such processes as MBE chamber bakeout, for instance. Also, with regard to phosphorus in particular, the use of white phosphorus, as opposed to red phosphorus<sup>12</sup> as source material would be more ideal in terms of flux stability.

The objective of the work reported in this article was to investigate phosphorus doping of ZnSe during MBE growth using an atomic phosphorus source designed specifically with elemental phosphorus handling in mind.

## II. CHARACTERIZATION OF ATOMIC PHOSPHORUS SOURCE

The phosphorus source employed in this work was manufactured by Oxford Applied Research and is a modified valved thermal cracker source design. A schematic of the source is illustrated in Fig. 1. The modifications include the

<sup>a)</sup>Electronic mail: rpark@mse.ufl.edu

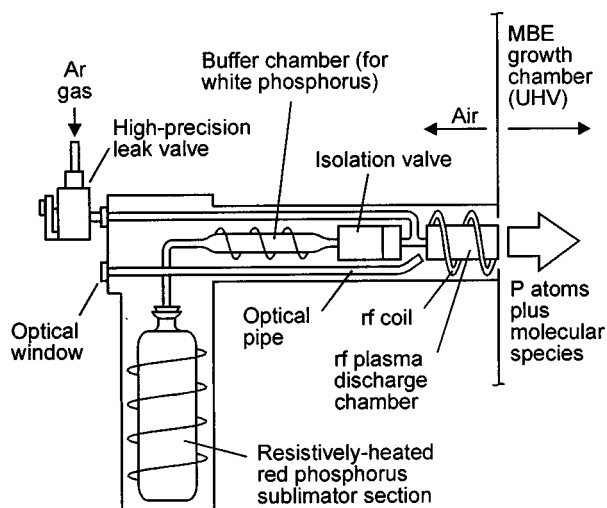


FIG. 1. Schematic of the atomic phosphorus source.

replacement of a conventional thermal cracker (dissociation) section by an rf plasma discharge chamber and the provision of a gas line feed to the discharge chamber. Also, as shown in the schematic, a light pipe and optical window are provided in order to allow monitoring of optical emission occurring in the plasma discharge chamber. The source of phosphorus that supplies phosphorus vapor ( $P_4$ ) to the rf plasma discharge chamber is white phosphorus, formed in the buffer chamber by the condensation of phosphorus vapors sublimed from red phosphorus in the sublimator section. White phosphorus is preferred over red phosphorus with regard to the provision of a stable  $P_4$  flux to the discharge section.<sup>17</sup> During operation of the source, the sublimator section was normally maintained at room temperature, although some runs were performed with direct heating to the sublimator in the range of 50–60 °C. The buffer chamber (white phosphorus source) temperature was typically around 75 °C during plasma discharge operation, since the buffer chamber attained this temperature (with no direct heating) by virtue of heat transfer from the high temperature plasma discharge chamber. The  $P_4$  flux supply to the discharge chamber was controlled via the isolation valve shown in the schematic.

### A. "Pure" phosphorus plasmas

A "pure" phosphorus plasma could be obtained in the discharge chamber by first striking an argon plasma and allowing the discharge to stabilize. Following argon plasma stabilization, a  $P_4$  flux could be introduced via the isolation valve and, through a constant process of adjustments to the rf source impedance matching network (not shown in the figure), a pure phosphorus plasma could be stabilized by gradually eliminating the argon gas supply.

Optical emission occurring in the plasma discharge chamber was monitored using a fiber-optic cable and personal computer-based plug-in expansion board spectrometer having a 1024-element charge coupled detector (CCD) a 600-line grating and a spectral range of 490–1012 nm.

A typical emission spectrum recorded from a pure phosphorus plasma is shown in Fig. 2(a). For comparison pur-

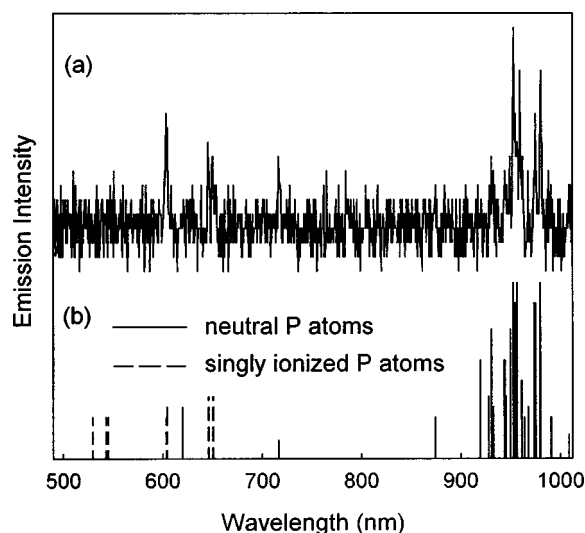


FIG. 2. (a) A typical atomic phosphorus optical emission spectrum recorded from a pure phosphorus plasma. (b) Spectrum of atomic phosphorus emission lines reported in the literature.

poses, Fig. 2(b) illustrates the spectrum of atomic phosphorus emission lines reported in the literature.<sup>18</sup> As can be seen from Figs. 2(a) and 2(b), the pure phosphorus plasma appears to be dominated by emission associated with neutral phosphorus atoms. In addition, lines associated with singly ionized phosphorus atoms are also evident. Consequently, the source appears eminently capable of generating a flux of atomic phosphorus. (The particular rf forward power employed in this case was 350 W, and the buffer chamber and sublimator temperatures were 100 and 25 °C, respectively.)

### B. Mixed argon-plus-phosphorus plasmas

Mixed plasmas were generated in the same fashion as described above for pure phosphorus plasmas except that in the mixed plasma case the argon gas was not eliminated from the discharge chamber.

Figure 3(a) shows a typical emission spectrum recorded from a mixed argon-plus-phosphorus plasma. Also shown for comparison purposes are the spectra of atomic argon [Fig. 3(b)] and atomic phosphorus [Fig. 3(c)] emission lines reported in the literature.<sup>18</sup> The mixed plasma emission spectrum [Fig. 3(a)] appears to be a superposition of atomic argon and atomic phosphorus emission lines, suggesting that the source in this case generates argon atoms and phosphorus atoms simultaneously. (Again, the rf forward power employed was 350 W, and the buffer chamber and sublimator temperatures were 100 and 25 °C, respectively.)

Higher still phosphorus concentrations were obtained in ZnSe films when direct heating (in the range of 50–60 °C) was applied to the sublimator chamber of the source. In the case of direct heating of the sublimator, the optical emission characteristics of mixed argon-plus-phosphorus plasmas were similar to those of mixed plasmas with the sublimator maintained at room temperature. However, the integrated emission intensity associated with the atomic phosphorus

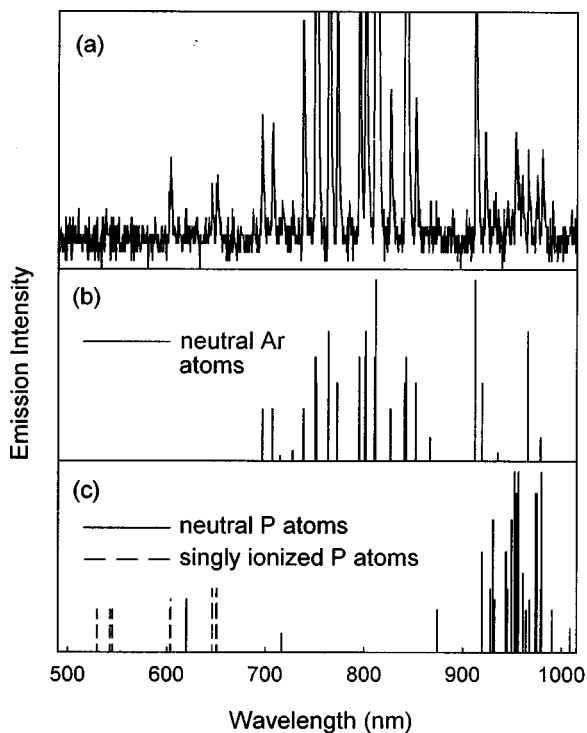


FIG. 3. (a) A typical optical emission spectrum recorded from a mixed argon-plus-phosphorus plasma using the same source operating conditions as in Fig. 2. Also shown for comparison are the emission lines reported in the literature for (b) atomic argon, and (c) atomic phosphorus.

lines was higher in the case of direct sublimator heating, which suggests that higher atomic fluxes were produced in these cases. We believe that the higher atomic phosphorus flux levels (which produced higher ZnSe:P doping concentrations) were a consequence of a higher  $P_4$  flow rate into the discharge chamber when the sublimator chamber was heated during source operation.

As discussed below, secondary ion mass spectrometry analysis was performed on a number of samples grown in this study, and as illustrated in Fig. 4, a correlation was found between the phosphorus concentration in the ZnSe epilayers and the integrated atomic phosphorus emission inten-

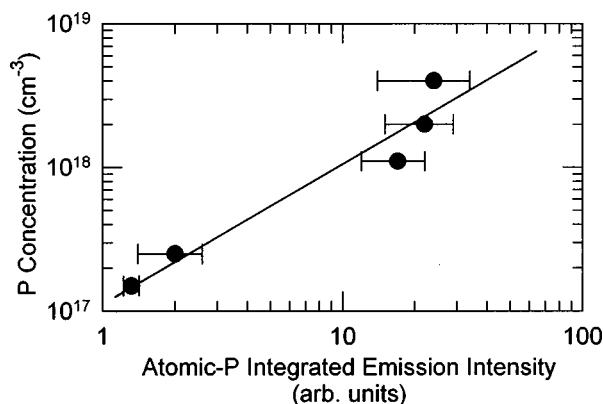


FIG. 4. A plot of phosphorus concentrations in ZnSe films vs the integrated atomic phosphorus emission intensities in the discharge chamber of the phosphorus source.

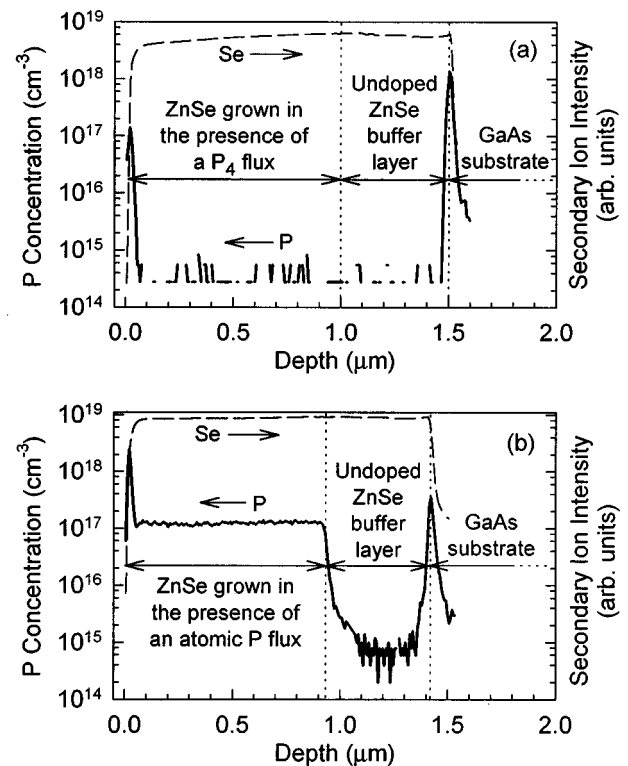


FIG. 5. SIMS depth profiles recorded from ZnSe films grown (a) in the presence of a  $P_4$  molecular flux (no rf power supplied to the cracker unit), and (b) in the presence of an atomic phosphorus flux generated in a pure phosphorus plasma (200 W rf forward power). In both cases the growth conditions and the buffer chamber and sublimator temperatures were the same.

sity in the plasma discharge chamber, as determined from optical emission spectra recorded during growth.

### III. SECONDARY ION MASS SPECTROMETRY ANALYSIS OF ZnSe:P FILMS

ZnSe films were grown by MBE on (100)-GaAs substrates under a variety of phosphorus source operating conditions and film growth conditions and were characterized using secondary ion mass spectrometry (SIMS) depth profiling analysis, particularly with regard to determining the phosphorus concentrations in the films. Conventional thermal effusion sources were employed for Zn and Se and in all cases a  $0.5\text{-}\mu\text{m}$ -thick unintentionally doped ZnSe buffer layer was grown prior to phosphorus doping. The MBE system used in this study was previously employed to grow nitrogen-doped ZnSe using an atomic nitrogen source.<sup>13</sup> SIMS analysis was performed at Charles Evans and Associates using a Cameca system ( $Cs^+$  primary ion beam).

Figures 5(a) and 5(b) illustrate SIMS depth profiles recorded from ZnSe films grown in the presence of a  $P_4$  molecular flux (no rf power supplied to the discharge chamber) and in the presence of an atomic phosphorus flux generated in a pure phosphorus plasma (an rf forward power of 200 W was supplied to the discharge chamber), respectively. In both cases the white phosphorus (buffer chamber) temperature was  $75^\circ\text{C}$ . Also, in both cases the growth conditions were

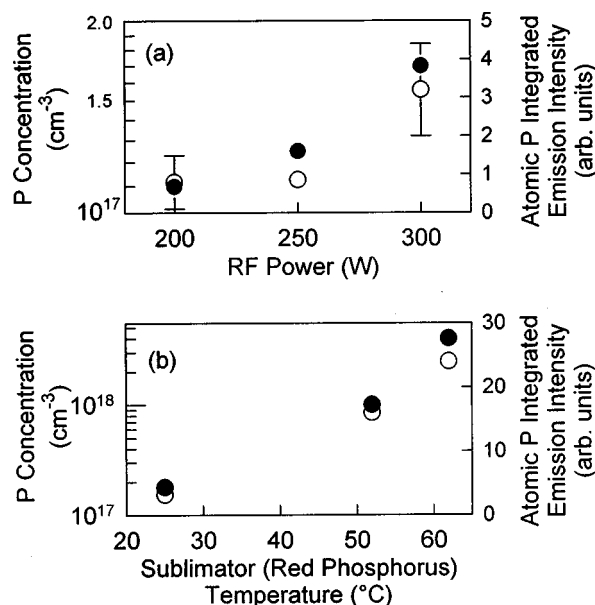


FIG. 6. Influence of source operating conditions on the phosphorus concentration (closed circles) in ZnSe films grown under a fixed set of growth conditions. The phosphorus concentration in the films is plotted (a) against the rf forward power applied to the discharge chamber of the source for a fixed sublimator temperature of 25 °C, and (b) against the sublimator temperature for a fixed rf forward power of 350 W. Also shown are the normalized integrated atomic phosphorus emission intensities (open circles).

the same, namely a growth temperature of 300 °C and a Se/Zn beam equivalent pressure ratio of 2.

As can be seen from these profiles, phosphorus is only incorporated into ZnSe during MBE under these conventional conditions when supplied as atomic, rather than molecular, phosphorus. The phosphorus concentration was below the SIMS detection limit ( $\sim 10^{15} \text{ cm}^{-3}$ ) when a P<sub>4</sub> molecular flux was supplied. Consequently, these data suggest a much higher chemical reactivity at the growing ZnSe surface for phosphorus atoms compared with P<sub>4</sub> molecules. The phosphorus concentration spikes at the film surface and ZnSe/GaAs heterointerface are believed to be SIMS artifacts.

The integrated atomic phosphorus emission intensity and, consequently, the phosphorus doping concentration can be varied by varying certain source parameters. For instance the rf forward power applied to the discharge chamber has the effect shown in Fig. 6(a), namely that an increase in the rf forward power produces an increase in the plasma emission intensity and, therefore, an increase in the phosphorus doping concentration in ZnSe films. As Fig. 6(b) illustrates, the sublimator temperature has an even greater influence on the integrated atomic phosphorus emission intensity and therefore, the phosphorus doping concentration (for a fixed rf forward power, 350 W in this case). The growth conditions employed for the experiments were the same, namely, a growth temperature of 300 °C and a Se/Zn beam equivalent pressure ratio of 2.

The phosphorus doping concentrations in ZnSe films were also found to depend significantly on growth parameters when the source operating conditions were maintained constant. Figures 7(a) and 7(b) illustrate the phosphorus doping concentration dependence on growth temperature and

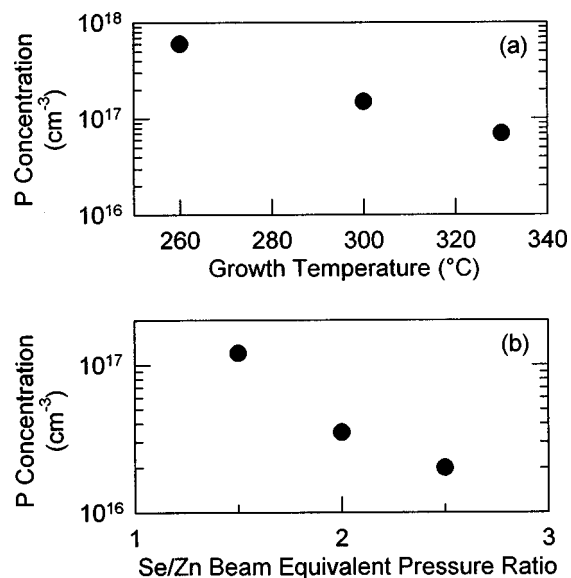


FIG. 7. Influence of growth conditions on the phosphorus concentration in ZnSe films grown using a fixed set of phosphorus source operating conditions. The phosphorus concentration in the films is plotted (a) against growth temperature, and (b) against Se/Zn beam equivalent pressure ratio.

Se/Zn beam equivalent pressure ratio employed during growth, respectively. The growth temperature dependence [Fig. 7(a)] suggests a temperature dependence for the atomic phosphorus sticking coefficient in the temperature range examined (260–330 °C), while the VI/II ratio dependence [Fig. 7(b)] suggests Zn–P and Zn–Se reactions to be competitive. We have previously determined that a Se/Zn beam equivalent pressure ratio of 2 produces near-stoichiometric ZnSe at a growth temperature of 300 °C. For these experiments, the phosphorus source operating conditions were a forward power of 200 W and buffer chamber and sublimator temperatures of 75 and 25 °C, respectively.

The highest quality ZnSe films (as evidenced by photoluminescence analysis) were grown at a substrate temperature of 300 °C and using a Se/Zn beam equivalent pressure ratio of 2, and consequently, this fixed set of growth conditions was employed to examine the influence of phosphorus concentration on the photoluminescence of ZnSe:P films.

#### IV. PHOTOLUMINESCENCE ANALYSIS OF ZnSe:P FILMS

A set of atomic-phosphorus-doped ZnSe films having phosphorus concentrations (determined by SIMS analysis) in the range of  $1 \times 10^{16}$  to  $1 \times 10^{18} \text{ cm}^{-3}$ , were characterized using low-temperature (13 K) photoluminescence (PL) analysis performed at the 3M Company, St. Paul, MN. The ZnSe:P films, which were 1  $\mu\text{m}$  thick and deposited on 0.5- $\mu\text{m}$ -thick undoped ZnSe buffer layers, were grown using a fixed set of growth conditions, namely a growth temperature of 300 °C and a Se/Zn beam equivalent pressure ratio of 2. The PL analysis was performed using the 361 nm line from an argon-ion laser (incident power density on the samples was 2 mW/cm<sup>2</sup>) and a detection system comprising a SPEX (1 meter) wavelength spectrometer (1800 grooves/mm grating) and a GaAs-based photomultiplier tube.

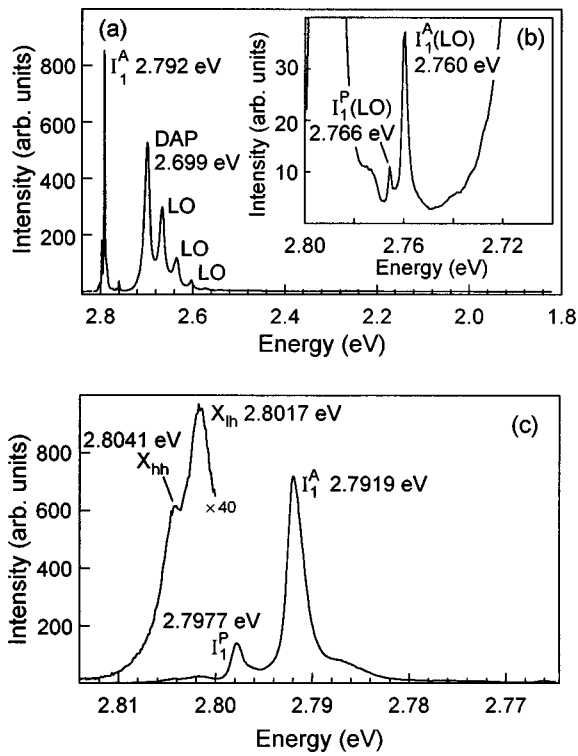


FIG. 8. Low-temperature (13 K) PL spectra recorded from a ZnSe:P film having a phosphorus concentration of  $1 \times 10^{16} \text{ cm}^{-3}$ . Note the dominance of the acceptor-bound exciton peak  $I_1^A$ . A strong longitudinal-optical phonon replica of the  $I_1^A$  peak is also evident [spectrum (b)].

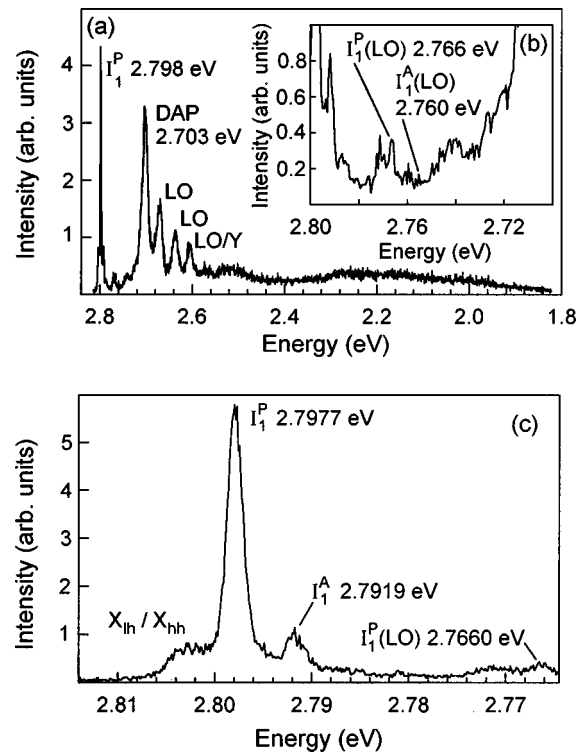


FIG. 10. Low-temperature (13 K) PL spectra recorded from a ZnSe:P film having a phosphorus concentration of  $1.5 \times 10^{17} \text{ cm}^{-3}$ . Note the absence of strong deep level emission in spectrum (a).

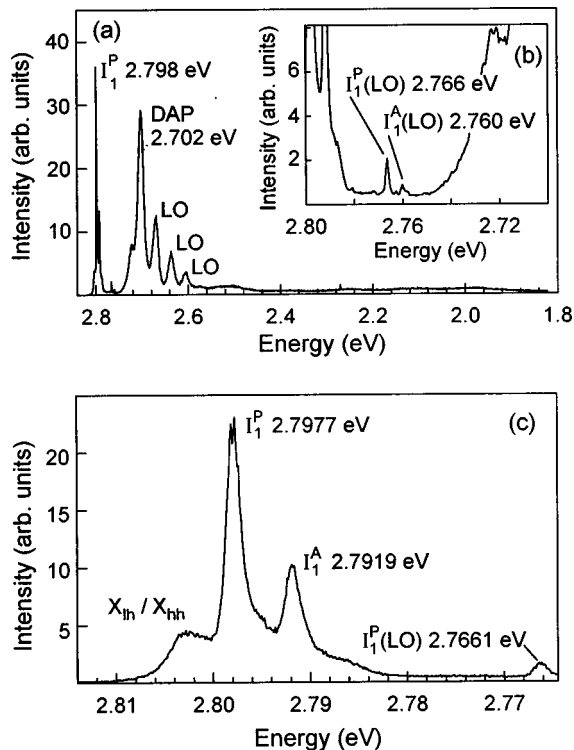


FIG. 9. Low-temperature (13 K) PL spectra recorded from a ZnSe:P film having a phosphorus concentration of  $3.5 \times 10^{16} \text{ cm}^{-3}$ . Note the dominance of the traditional phosphorus-related acceptor-bound exciton peak,  $I_1^P$ , over the  $I_1^A$  acceptor-bound exciton peak at this doping concentration.

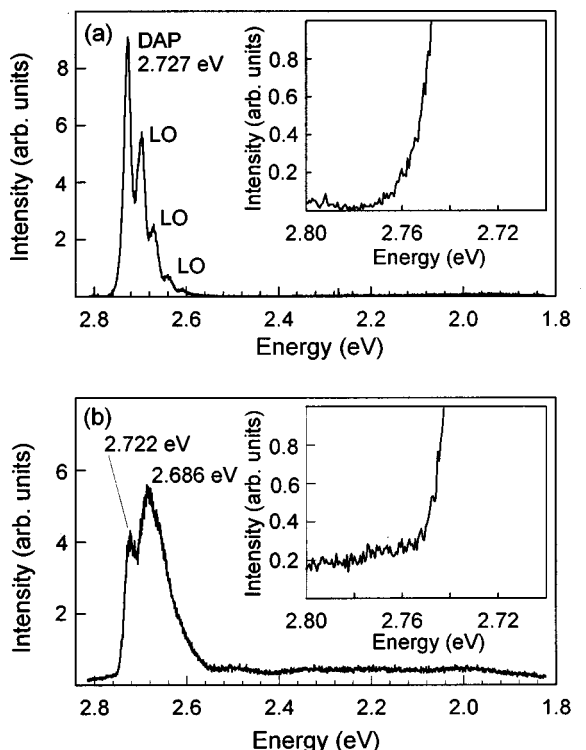


FIG. 11. Low-temperature (13 K) PL spectra recorded from ZnSe:P films. The phosphorus concentrations in the films were (a)  $3 \times 10^{17}$  and (b)  $1 \times 10^{18} \text{ cm}^{-3}$ . Again, note the absence of strong deep level emission in these spectra.

TABLE I. Photoluminescence emission peak identification labels used in this work.

Label	Peak assignment
$X_{nh}$	Heavy-hole free exciton
$X_{lh}$	Light-hole free exciton
$I_2$	Neutral donor-bound exciton
$I_1^P$	Phosphorus doping related exciton
$I_1^A$	Acceptor-bound exciton associated with atomic-phosphorus doping
$I_1^P$ (LO)	LO-phonon replica of $I_1^P$
$I_1^A$ (LO)	LO-phonon replica of $I_1^A$
DAP	Donor-to-acceptor pair (zero-phonon) transition
LO	LO-phonon replica of donor-to-acceptor pair transition

Figures 8, 9, and 10, illustrate PL spectra recorded from ZnSe films having phosphorus concentrations of  $1 \times 10^{16}$ ,  $3.5 \times 10^{16}$ , and  $1.5 \times 10^{17} \text{ cm}^{-3}$ , respectively, while Fig. 11 shows PL spectra recorded from films having phosphorus concentrations of  $3 \times 10^{17}$  and  $1 \times 10^{18} \text{ cm}^{-3}$ .

The PL peak assignments indicated in the various PL spectra are specified in Table I.

The variously assigned PL peaks have been well documented in the literature with regard to phosphorus doped ZnSe (for a review, see Ref. 19) with the exception of the peak that we have labeled as  $I_1^A$ , which was recently identified by Neu *et al.*<sup>12</sup> and which is dominant in the PL spectrum recorded from the sample having the lowest phosphorus concentration ( $[P]=1 \times 10^{16} \text{ cm}^{-3}$ , see Fig. 8). It is interesting to note that at higher phosphorus concentrations, namely  $3.5 \times 10^{16}$  and  $1 \times 10^{17} \text{ cm}^{-3}$ , the  $I_1^P$  peak dominates the excitonic emission range (see Figs. 9 and 10) while the  $I_1^A$  peak emission intensity is diminished. Analysis of the  $I_1^P$  and  $I_1^A$  peaks is provided in Sec. VI.

Donor-to-acceptor pair (DAP) transitions are also evident in the ZnSe:P PL spectra, suggesting compensation by relatively shallow donors. Indeed, DAP emission dominates the spectra recorded from the more heavily doped films (Fig. 11). It is interesting to note that the energy of the zero-phonon DAP transition is higher by about 25 meV in the case of the more heavily doped films ( $[P] \geq 3 \times 10^{17} \text{ cm}^{-3}$ , Fig. 11) compared to the energy of the zero-phonon transition in the lighter doped films (see Figs. 8–10). It is tempting to conclude that a deeper acceptor, which is assumed to provided the  $I_1^A$  acceptor-bound exciton emission, participates in the DAP (lower energy transitions) in the case of the lighter doped material while the shallower acceptor, assumed to be responsible for the  $I_1^P$  emission, dominates in the case of the higher energy DAP transitions occurring in the more heavily doped films, although this would only be speculation at this stage.

It is also interesting to note the absence of significant deep-level emission in any of the presented PL spectra. Previous authors<sup>8,10,20</sup> have speculated that deep levels in ZnSe:P films are a natural consequence of heavy phosphorus doping, however, as can be seen from Fig. 11, significant deep-level emission was not observed even in PL spectra recorded from atomic phosphorus-doped ZnSe films having phosphorus concentrations as high as  $10^{18} \text{ cm}^{-3}$ . Conse-

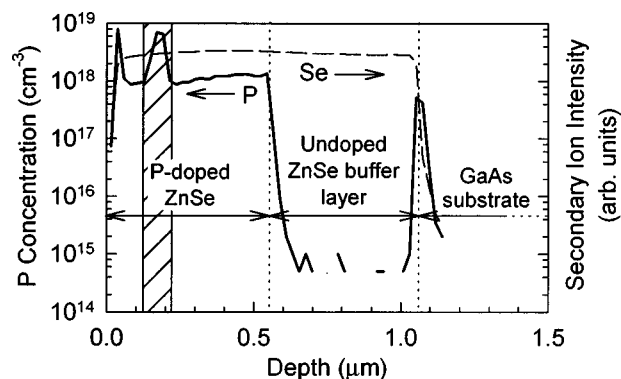


FIG. 12. SIMS depth profile recorded from an atomic phosphorus-doped ZnSe sample grown using two different growth modes. The majority of the film was grown using conventional molecular beam epitaxy (MBE) under a fixed set of source operating conditions and growth conditions. However, 1000 Å of the film (shaded area) was grown using an alternate element exposure (AEE) growth mode rather than MBE, with the atomic phosphorus source operating conditions remaining fixed.

quently, it can be concluded that deep-level formation is not intrinsic to the ZnSe:P system as previously thought. All of the ZnSe:P films grown in this study, however, were electrically insulating. Since compensation by deep states does not seem likely in our material, it appears that compensation by relatively shallow donors prevents significant free-carrier production in ZnSe:P films grown using the atomic phosphorus source.

## V. DEPENDENCE OF PHOSPHORUS CONCENTRATION ON GROWTH MODE

With a view to promoting and enhancing Zn–P reactions at the growing surface, a particular growth mode, which we term “alternate element exposure” (AEE), was employed. During AEE growth of ZnSe:P the Zn, Se, and atomic P source shutters were operated in a particular fashion in order to produce the following flux exposure sequence (to the wafer) during a single cycle of growth: 2 s Zn flux exposure, 1 s delay (no exposure), 5 s atomic P flux exposure, 7 s Se plus atomic P fluxes exposure, and 1 s delay (no exposure).

In a particular experiment the above sequence was repeated a total of 707 times in order to deposit 1000 Å of ZnSe:P (each cycle produced 0.5 monolayer of growth). Since Se and P compete with each other for reaction with available Zn, the idea behind the above flux exposure sequence was to allow P to react with Zn initially in the absence of Se.

Figure 12 illustrates a SIMS depth profile recorded from an atomic phosphorus-doped ZnSe film grown using two different growth modes. The majority of the film was grown using conventional MBE under a fixed set of atomic phosphorus source operating conditions [rf forward power=200 W, white phosphorus source temperature (buffer chamber temperature)=75 °C, and a sublimator temperature of 50 °C] and a fixed set of growth conditions (growth temperature =300 °C and Se/Zn beam equivalent pressure ratio=2). However, 1000 Å of the film was grown using the alternate element exposure mode of growth described above rather than MBE, with the atomic phosphorus source operating

conditions remaining fixed, i.e., the atomic P flux level was not changed. The shaded region in the SIMS profile (Fig. 12) represents the AEE portion of the growth. As can be seen from the figure, the MBE growth mode produced a phosphorus concentration around  $10^{18} \text{ cm}^{-3}$ , however, almost an order of magnitude higher phosphorus concentration was obtained using the AEE mode of growth. Consequently, higher phosphorus doping levels can be obtained in ZnSe (for a given atomic P flux level) by suitably promoting Zn–P reactions.

## VI. DISCUSSION

The nature of the phosphorus-related acceptor in ZnSe has been the subject of much discussion in the literature. Some authors have speculated that phosphorus is not simply incorporated substitutionally on a selenium sublattice site but rather is a complex involving phosphorus, such speculation being based on the deep level emissions observed in some studies,<sup>5</sup> and on the relatively shallow localization energy and the absence of strain splitting exhibited by the  $I_1^P$  peak.<sup>19</sup> Zhang *et al.*,<sup>21</sup> relying on selective PL (SPL) analysis of the excited states of the common, known acceptors in ZnSe, added to this speculation by asserting that the P-related acceptor in ZnSe, unlike the other shallow acceptors, does not follow effective mass theory and, hence, may involve a complex. On the other hand, Neu *et al.*<sup>12</sup> contend that the SPL data reported by Zhang *et al.* are incomplete. Based on their own data, Neu *et al.* assert that, in fact, none of the common shallow acceptors in ZnSe, including phosphorus, follow effective mass theory.

Adding to this debate is the lack of agreement on how to interpret the PL spectra recorded from phosphorus-doped ZnSe. Bhargava<sup>22</sup> first proposed the  $I_1^P$  peak to be an acceptor-bound exciton related to phosphorus doping. Prior to Bhargava's proposal, this peak had been identified as a neutral donor-bound exciton peak, an understandable assignment given the region of the PL spectra in which the  $I_1^P$  peak is located. The location of the  $I_1^P$  peak in a relatively high-energy region indicates that the exciton giving rise to this peak is bound to an acceptor having an unusually low ("shallow") localization energy, assuming that it is, in fact, acceptor related.

Bhargava<sup>22</sup> supported his argument that the  $I_1^P$  peak is associated with an acceptor rather than a donor by citing the presence of another peak located approximately 32 meV lower in energy. This peak was identified as an longitudinal optical (LO)-phonon replica of  $I_1^P$ , the LO-phonon energy in ZnSe being around 32 meV. This peak is listed in Table I as  $I_1^P$  (LO) and is present in the PL spectra shown in Figs. 8–10. Bhargava based his argument on the intensity of  $I_1^P$  (LO) relative to that of  $I_1^P$ , suggesting that the  $I_1^P$  (LO)/ $I_1^P$  ratio should be approximately 0.03 for shallow acceptors. Indeed, the  $I_1^P$  (LO)/ $I_1^P$  intensity ratio observed in the PL spectra recorded in this work appears to be approximately 0.03.

Zhang *et al.*<sup>23</sup> have concurred with Bhargava's assignment and have offered further evidence that the  $I_1^P$  peak is associated with an acceptor-bound exciton by drawing atten-

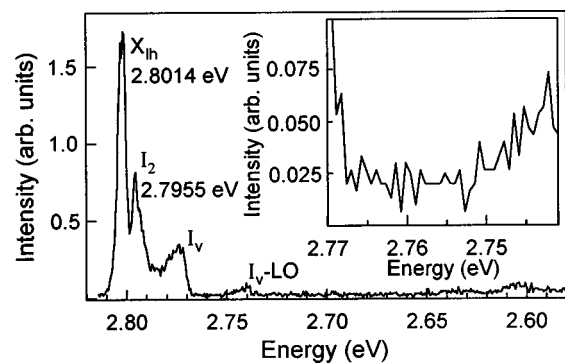


FIG. 13. Low-temperature (13 K) PL spectra recorded from an unintentionally doped ZnSe film showing a neutral donor-bound exciton peak,  $I_2$ , at 2.7955 eV. Note the absence of a strong phonon replica, which would appear at 2.7635 eV if present.

tion to what they referred to as the "undulation wing," a relatively weak, gently sloping shoulder occupying an energy range of approximately 4 meV on the low-energy side of  $I_1^P$ . As described by Zhang *et al.*,<sup>23</sup> the undulation wing is thought to be associated with the emission of excitons bound to pairs of shallow acceptors separated by various distances.

The PL spectra recorded in this study also exhibited an undulation wing on the low-energy side of  $I_1^P$ , however, the undulation wing in the PL spectra recorded from these samples is dominated by a distinct, relatively intense peak, labeled  $I_1^A$  in Table I and in Figs. 8–10. The  $I_1^A$  peak, first reported by Neu *et al.*,<sup>12</sup> but termed  $I_1^P$ , may also be present in the spectra reported by Zhang *et al.*<sup>23</sup> but only in the form of a hump on the undulation wing. A similar hump is present in the PL spectra recorded by Yao and Okada<sup>9</sup> from their MBE-grown ZnSe:P. Interestingly, the  $I_1^A$  peak became less intense in the PL spectra recorded in this present study as the phosphorus concentration increased; however in all cases the  $I_1^A$  peak is the dominant feature in the undulation wing region of the spectra. Indeed, it is the dominant peak in the overall PL spectrum recorded from the most lightly doped sample ( $[P]=1 \times 10^{16} \text{ cm}^{-3}$ , Fig. 8).

The  $I_1^A$  peak is located in a region of the ZnSe PL spectrum that is commonly occupied by neutral acceptor-bound exciton emission peaks, and as in the case of the undulation wing reported by Zhang *et al.*,<sup>23</sup> the  $I_1^A$  peak is accompanied by a relatively strong LO-phonon replica [see Fig. 8(b)], suggesting that the  $I_1^A$  peak represents an acceptor-bound exciton transition, following the reasoning of Bhargava.

The PL spectra recorded by Neu *et al.* from their ZnSe:P samples exhibited a peak similar to  $I_1^P$  (our label) with an associated strong phonon replica. However, their unintentionally doped ZnSe sample, having a net electron concentration ( $N_d - N_a$ ) of  $\sim 5 - 10 \times 10^{14} \text{ cm}^{-3}$ , exhibited a peak that these authors assumed to be a neutral donor-bound exciton peak ( $I_2$ ), and it too was accompanied by a strong phonon replica. Based on these observations, Neu *et al.* question Bhargava's analysis and suggest that  $I_1^P$  (our label) is actually a phosphorus-related donor bound, rather than acceptor bound, exciton peak, in spite of the strength of the phonon replica. Neu *et al.* appear to indicate that  $I_2$  (their label) is present in the PL spectra recorded from both their

undoped and P-doped samples and that phosphorus doping does not produce a new peak in the vicinity of  $I_2$ .

By contrast, as Fig. 13 illustrates, the PL spectra recorded from our own unintentionally doped ZnSe samples do not exhibit a strong phonon replica associated with the native donor-bound exciton transition,  $I_2$ . In addition,  $I_1^P$  and  $I_2$  in the present work appear at different energies, approximately 2.7977 and 2.7955 eV, respectively. Consequently, our contention is that the  $I_1^P$  peak is phosphorus doping related and may well be related to an acceptor-type defect, while the new  $I_1^A$  peak certainly relates to an acceptor-type level associated with phosphorus doping.

## VII. CONCLUSIONS

The following conclusions are drawn from this work:

- (1) The Oxford Applied Research valved solid-source rf cracker unit is eminently suitable for the provision of an atomic phosphorus flux for MBE growth.
- (2) Phosphorus atoms are exceedingly more chemically reactive at a growing ZnSe surface (growth temperature around 300 °C) than are  $P_4$  molecules.
- (3) Solid solubility is not a limiting factor with regard to ZnSe:P since phosphorus concentrations approaching  $10^{19} \text{ cm}^{-3}$  were obtained (probably not an upper limit) using the atomic phosphorus source.
- (4) Doping using atomic phosphorus appears, at least in lightly to moderately doped ZnSe, to provide an acceptor state that has a localization energy (as judged from the acceptor-bound exciton energy) more in keeping with that of simple substitutional acceptors in ZnSe.
- (5) Compensation in ZnSe:P does not occur intrinsically from deep level defects but rather by virtue of the formation of shallow donor states since at higher phosphorus concentrations in our atomic P-doped ZnSe films, DAP transitions dominate the PL spectra rather than deep-level emission.

Finally, although  $p$ -type conductivity in ZnSe does not appear feasible using phosphorus even when supplied as atomic phosphorus, we believe that atomic phosphorus fluxes could be employed successfully in other application areas such as MBE growth of phosphide compounds (low-temperature growth) and phosphorus ( $n$ -type) doping of Si (again, low-temperature epitaxial growth), for instance.

## ACKNOWLEDGMENTS

The authors wish to thank Greg Meis-Haugen and Dr. Michael Haase of the 3M Company (St. Paul, MN) for the PL measurements and for facilitating the SIMS measurements. Also, their interest in this project was much appreciated. Financial support from the 3M Company made this work possible. We would also like to thank Oxford Applied Research personnel for their unwavering cooperation with regard to the atomic phosphorus source design.

- <sup>1</sup>W. C. Holton, R. K. Watts, and R. D. Stinedurf, *J. Cryst. Growth* **6**, 97 (1969).
- <sup>2</sup>A. T. Reinberg, W. C. Holton, M. de Wit, and R. K. Watts, *Phys. Rev. B* **3**, 410 (1971).
- <sup>3</sup>R. K. Watts, W. C. Holton, and M. de Wit, *Phys. Rev. B* **3**, 404 (1971).
- <sup>4</sup>J. E. Nicholls and J. J. Davies, *J. Phys. C* **12**, 1917 (1979).
- <sup>5</sup>Y. S. Park and B. K. Shin, *J. Appl. Phys.* **45**, 1444 (1974).
- <sup>6</sup>K. Kosai, B. H. Fitzpatrick, H. G. Grimmeiss, R. N. Bhargava, and G. F. Neumark, *Appl. Phys. Lett.* **35**, 194 (1979).
- <sup>7</sup>B. J. Fitzpatrick, C. J. Werkhoven, T. J. McGee, P. M. Hardnack, S. P. Herko, and R. N. Bhargava, *IEEE Trans. Electron Devices* **ED-28**, 440 (1981).
- <sup>8</sup>W. Stutius, *Appl. Phys. Lett.* **40**, 246 (1982).
- <sup>9</sup>T. Yao and Y. Okada, *Jpn. J. Appl. Phys.* **25**, 821 (1986).
- <sup>10</sup>J. M. DePuydt, T. L. Smith, J. E. Potts, H. Cheng, and S. K. Mohapatra, *J. Cryst. Growth* **86**, 318 (1988).
- <sup>11</sup>K. Morimoto, *J. Cryst. Growth* **117**, 111 (1992).
- <sup>12</sup>G. Neu, C. Morhain, E. Tournié, and J. P. Faurie, *J. Cryst. Growth* **184/185**, 515 (1998).
- <sup>13</sup>R. M. Park, M. B. Troffer, C. M. Rouleau, J. M. DePuydt, and M. A. Haase, *Appl. Phys. Lett.* **57**, 2127 (1990).
- <sup>14</sup>Y. Fan, J. Han, L. He, J. Saraie, R. Gunshor, M. Hagerott, H. Jeon, A. Nurmikko, G. C. Hua, and N. Otsuka, *Appl. Phys. Lett.* **61**, 3160 (1993).
- <sup>15</sup>H.-J. Lugauer, A. Waag, L. Worschech, W. Ossau, and G. Landwehr, *J. Cryst. Growth* **161**, 86 (1996).
- <sup>16</sup>E. Tournié, C. Morhain, C. Ongaretto, V. Bousquet, P. Brunet, G. Neu, J.-P. Faurie, R. Triboulet, and J. O. Ndap, *Mater. Sci. Eng., B* **43**, 21 (1997).
- <sup>17</sup>F. G. Johnson and C. E. C. Wood, *J. Appl. Phys.* **78**, 1664 (1995).
- <sup>18</sup>J. Reader and C. H. Corliss, in *CRC Handbook of Chemistry and Physics*, edited by David R. Lide (Chemical Rubber, Cleveland, 1993), pp. 10-1-10-90.
- <sup>19</sup>B. J. Skromme, in *Annual Review of Materials Science*, edited by E. N. Kaufmann (Annual Review, Palo Alto, 1995), pp. 601-646.
- <sup>20</sup>D. J. Chadi and K. J. Chang, *Appl. Phys. Lett.* **55**, 575 (1989).
- <sup>21</sup>Y. Zhang, W. Liu, B. J. Skromme, H. Cheng, S. M. Shibli, and M. C. Tamargo, *J. Cryst. Growth* **138**, 310 (1994).
- <sup>22</sup>R. N. Bhargava, *J. Cryst. Growth* **86**, 873 (1988).
- <sup>23</sup>Y. Zhang, B. J. Skromme, and H. Cheng, in *Semiconductor Heterostructures for Photonic and Electronic Applications*, edited by D. C. Houghton, C. W. Tu, and R. T. Tung (Materials Research Society, Pittsburgh, 1993), pp. 567-572.